IEEE Access
Multidisciplinary | Rapid Review | Open Access Journal

Received August 29, 2018, accepted October 7, 2018, date of publication October 22, 2018, date of current version November 30, 2018.

Digital Object Identifier 10.1109/ACCESS.2018.2877254

Recognition of Chronic Low Back Pain During Lumbar Spine Movements Based on Surface Electromyography Signals

WENJING DU[1]*, OLATUNJI MUMINI OMISORE[1,2]*, HUIHUI LI[1], KAMEN IVANOV[1,2], SHIPENG HAN[1], AND LEI WANG[1]

[1]Key Laboratory for Low-Cost Healthcare, Shenzhen Institutes of Advanced Technology, Chinese Academy of Sciences, Shenzhen 518055, China
[2]Shenzhen College of Advanced Technology, University of Chinese Academy of Sciences, Shenzhen 518055, China

*Wenjing Du and Olatunji Mumini Omisore are Co-First Authors

Corresponding author: Lei Wang (wang.lei@siat.ac.cn; wang_siat@163.com)

This work was supported in part by the National Natural Science Foundation of China under Grant 61501445 and Grant U1505251, in part by the Applied Project for Scientific and Technological Research and Development under Grant 2015B020233004, and in part by the Foundation of Public Technology Service Platform of Biomedical Electronics.

ABSTRACT Chronic low back pain (CLBP) is a common musculoskeletal disorder and a major source of disability in adults. The assessment of lumbar muscle functioning has proven as an appropriate approach for early identification of CLBP when significant pathological signs and symptoms are absent. Thus, earlier therapy or rehabilitation can be administered to prevent further deterioration, such as spinal stenosis or disk herniation. In this paper, surface electromyography (sEMG) signal analysis was explored for the recognition of low back pain in subjects with non-specific symptoms; 88 CLBP subjects and a control group of 83 subjects were recruited for sEMG data acquisition. Subjects were asked to perform four specific movements, namely forward bending, backward bending, right lateral flexion, and left lateral flexion. While performing each movement, sEMG signals from three pairs of lumbar muscles were captured, and 31 features from both the time and frequency domains were extracted from the signal. Finally, the main feature group and four subsets, derived from it, were explored. The suggested method allowed to achieve CLBP recognition accuracy of 98.04% based on subset C for forward bending, followed by 96.15% based on subset E for right lateral flexion, 93.33% based on subset E for left lateral flexion, and 91.30% based on subset B for backward bending. A combination of support vector machine classifiers and optimal feature selection allowed for improved classification performance. The main aim of this paper is to recognize CLBP in subjects with non-specific pathology during the four types of movement. The major steps carried out to achieve this are pre-processing, feature selection, and classification of the sEMG signals acquired from 171 subjects. Results suggest CLBP recognition based on sEMG as a promising alternative to the conventional methods. Therefore, this paper could inspire the design of appropriate programs that can ensure effective rehabilitation of CLBP patients.

INDEX TERMS Chronic low back pain, lumbar muscle function, surface electromyography, recognition accuracy.

I. INTRODUCTION

Nowadays, low back pain (LBP) is a common phenomenon in human beings, and most of its occurrence comes as a result of overuse or strain of the spine. However, chronic low back pain (CLBP) is a serious mental condition in which people with LBP persists for more than three months in people with mild or acute symptoms. Recently, this mental condition features a high prevalence in developed and business-oriented countries with approximately, 3 out of 10 people been affected in the US [1]–[3]. Previous studies have shown that CLBP is one of the most common causes of increased disability rates, which, as a consequence, leads to a high leave of absence from work in some countries [4]–[6]. The increased prevalence of people with LBP would seem to depend on two reasons: the high treatment cost and the lack of adequate early screening procedure. Nonetheless, the gradual development of biomedical technology, physiological signal processing is becoming a way to better treatment approaches [7].

2169-3536 © 2018 IEEE. Translations and content mining are permitted for academic research only.
Personal use is also permitted, but republication/redistribution requires IEEE permission.
See http://www.ieee.org/publications_standards/publications/rights/index.html for more information.

The degree of LBP differs amongst people. Usually, it ranges from mild status, which is common in many people, to very severe levels in which the affected persons might be unable to make some spine movements. Nonetheless, most early back pain disorders can get better with simple rehabilitation programs administered with advice from health providers, such as a physiotherapist. These include exercises such as bending and stretching to strengthening muscles, counseling affected persons to understand some ways to manage their pains [8], [9]. However, lack of strict adherence to the guidelines can hasten translation of the mild status to numbness, weakness, or loss of movements.

In the case of severe back pain, medicine, epidural injection, or spinal surgery is needed to improve the health disorder, but these also have some side effects. For example, medications used for treating CLBP comes with side effects such as gastrointestinal disorders, ulcers, and kidney damage; especially when taken at higher doses for a long time [10]. Also, epidural injection and surgery can increase physical injury and pain experienced by patients during and after the procedure. These methods require treatment costs which can be very high in some cases [11], [12]. Moreover, previous studies also showed that delaying referral to medicine, epidural injection, or spinal surgery is associated with increased overall health care costs and higher risk for receiving advanced imaging or invasive procedures for CLBP [13], [14]. Thus, these methods come with economic burdens, one of the factors considered in treatment selection of CLBP [15]. According to Gore *et al.* [16], CLBP patients are characterized by greater comorbidity and economic burdens which can be attributed to prescription of more pain-related medications and increased utilization of health resources, compared with those without CLBP.

In previous literature, clinical diagnoses have shown that the typical signs of LBP include muscle weakness, dull aching pain, sharp pain, tingling or burning sensation [17]. Yet, 85% of CLBP disorders have no specific pathology and are, therefore, regarded as ''non-specific'' [1]. To verify the cause of back pain, techniques involving X-ray, Computed Tomography (CT) or magnetic resonance imaging (MRI) scans can be used to pinpoint the location of spinal damages such as stenosis, extra wear, and tear, or herniated disks. Further analysis can then be performed to figure out how the damage affects the person's movements. However, radiation from X-ray and CT methods can affect people's health while MRI scanning is very expensive. In addition, causes of pains cannot be found by the imaging methods if there are no apparent lesions. In current clinical evaluation methods, the latter has been addressed by pain scoring which is done by evaluating subjective opinions from the patient [18]. However, this method is limited because pain scores are generally completed by subjects [19] who might be anxious or depressed [20], [21]. Thus, the assessment can be highly biased and would not seem to reveal dysfunction location from pathophysiology of pain perception.

Some prospective studies revealed that understanding the pathophysiology of pain perception can be evaluated well by combining biomedical signals and psychological factors [22]–[24]. With this, a quantitative and objective method that can evaluate LBP and monitor rehabilitation of affected patients can be achieved. Besides, this can help physicians in diagnosing CLBP and acquiring comprehensive pathophysiological information to enhance regular treatments of LBP such that affected persons can recover sooner. Recently, there is growing interest in the use of real-time surface electromyography (sEMG) as a valid reference for treatment and rehabilitation of CLBP and as well, to assess lumbar stability muscle activities and functions [24], [25]. Some studies showed higher reliability and validity of real-time sEMG in assessing muscle activities during LBP evaluation, compared to other clinical methods [26]–[28]. In other studies [29], [30], changes in recruitment pattern of lumbar muscles, fiber distribution of paraspinal muscles, and cross-sectional area of lumbar multifidus muscles have been highlighted as contributory factors toward recurrent or chronic symptoms in people with LBP. In a related study [31], sEMG signals were quantified for clinical evaluation and characterization of LBP leading to disability in developing nations. Similarly, Du *et al.* [32] used sEMG signals to quantify the co-contraction performance of lumbar muscles between healthy subjects and patients with lumber disc herniation, which is a common CLBP. Signals acquired for both groups were explored to check if significant differences exist between subjects in the groups. According to Willigenburg *et al.* [33], these have impacts on movement trajectory of the lumbar spine such that lumbar dysfunction muscles provide relatively less protection for the lumbar spine. Thus, in this study, a recognition model is proposed for screening CLBP subjects with non-specific lumbar muscle pathology. The screening is based on analysis of thirty-one features obtained from sEMG signals that were acquired from three-pair muscles during execution of four specific types of lumbar movement. This is an important step towards earlier detection of CLBP in people without significant pathological symptoms. Thus, appropriate therapeutic or rehabilitation strategies can be implemented to prevent back pain deterioration.

II. METHODS

A. PARTICIPANTS

In this study, a total of 171 subjects were recruited from the department of local rehabilitation, Longgang Center Hospital (Shenzhen, China). From the subjects, 88 were CLBP patients who have suffered LBP for at least 3 months and not more than 12 months; before acquiring their sEMG data. Diagnoses of the 88 subjects confirmed no apparent pathological abnormality using CT or MRI scans. Furthermore, the subjects had no history of spinal surgery, lumbar spine, hip contractures, chronic pain pathology, respiratory disease, neurological disease or cardiac disease. Finally, the subjects have only used physical therapy to relieve their pain symptoms. At other side

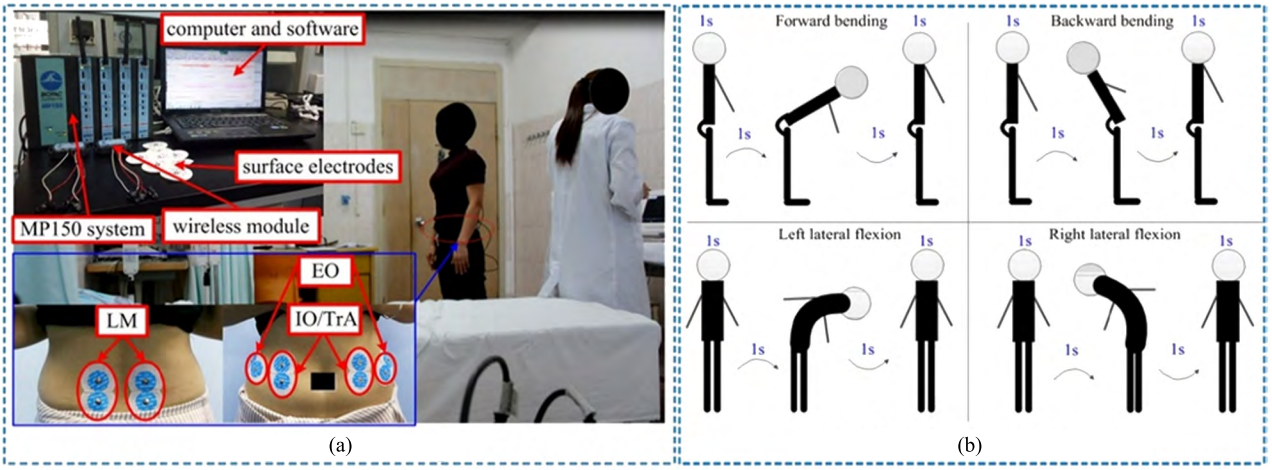

FIGURE 1. (a) Experimental setup, (b) the four types of movement.

of the spectrum, the remaining eighty-three subjects were healthy controls who had no history of LBP. The subjects in the control group were carefully chosen such that their gender, age, weight, height, and body mass index (BMI) matched those of the CLBP group. Details about subjects of both groups are presented in **Table1**.

TABLE 1. Details about subjects of both groups (means±SD).

	CLBP （n = 88） *(female n = 70, male n = 18)*	Control (n = 83) *female (n = 62, male n = 21)*	*p-value*
Age (years)	35.56 ± 7.28	34.27 ± 5.87	0.202
Age range (years)	21 ~ 50	24 ~ 49	/
Body weight (kg)	59.25 ± 9.18	59.30 ± 8.16	0.969
Body height (cm)	161.26 ± 6.90	163.00 ±7.41	0.114
BMI (kg/m^2)	17.21 ~ 36.39	17.85 ~ 34.22	/
BMI range (kg/m^2)	22.72 ± 2.78	22.32± 2.79	0.345
Pain VAS (0-10cm)	3.01 ± 1.31	/	/

SD - standard deviation, BMI- body mass index, VAS -visual analogue scale.

The experimental procedure was approved by the Institutional Review Board of Shenzhen Institutes of Advanced Technology (Reference No. SIAT-IRB-140215-H0037), and all the subjects signed informed consent forms before acquiring their signals and experiments. Sequel to signal acquisition, we carried out one-way analysis of variance (ANOVA) to determine whether there are significant differences ($p < 0.05$) between the mean for age and BMI of subjects in both groups. The statistical results obtained for the particular subjects are as presented in **Table 1**. Also, pain intensities of subjects in the CLBP group were evaluated using a Visual Analogue Scale (VAS) of 10 cm length, where 0 and 10 indicate no pain unbearable (but imaginable) pain.

B. EXPERIMENTAL DESIGN AND sEMG SIGNAL ACQUISITION

To acquire the desired signals, all participants were requested to perform four different types of movement which are: forward bending, backward bending, left lateral flexion and right lateral flexion. Each of the movements was performed five times repeatedly before continuing with the next movement. For each movement sequence, a separate sEMG recording was captured. Thus, a total of twenty sEMG recordings were acquired for each subject. All the subjects were ensured to have performed the required actions appropriately under the guidance of an examiner and an automated system. The latter produces a prerecorded rhythmic audio signal to ensure consistency in movement pace of the subjects. For readers' clarity, an illustration of the experimental setup is shown in **Figure 1a**. Each subject was asked to stand straight on a horizontal ground for one second with the hands kept down. The subjects were asked to follow a pre-recorded audio rhythm while making the movement sequence. This was done in order to ensure that the required movements are perfected. Each movement consisted of four sub-parts, namely: standing upright, bending forward, going back to standing position, and standing upright again. Each sub-part took approximately 1 second to execute. Thus, each subject performed the corresponding motions for about 4 seconds, after which he/she takes a rest for 30 seconds before proceeding to the next movement. Illustration of the movements and their subparts are as shown in **Figure 1b**.

According to clinical observations, subjects with CLBP have weaker lumbar muscles than healthy subjects, and as a result, they cannot perform large-degree flexion. Hence, subjects in the CLBP group were asked to try their best in completing the left and right lateral flexion movements until their pain gets high. Six pairs of surface electrodes (disposable Ag/AgCl, 10 mm diameter, LT-301, China), were placed on the subject's waist covering the muscles of interest: left and right external oblique (EO), lumbar multifidus (LM), and internal oblique/transversus abdominis (IO/TrA) muscles. As shown in Figure 1a, only one electrode pair was required to cover each pair IO/TrA muscles since the muscles pass through a common region around the human waist. In each

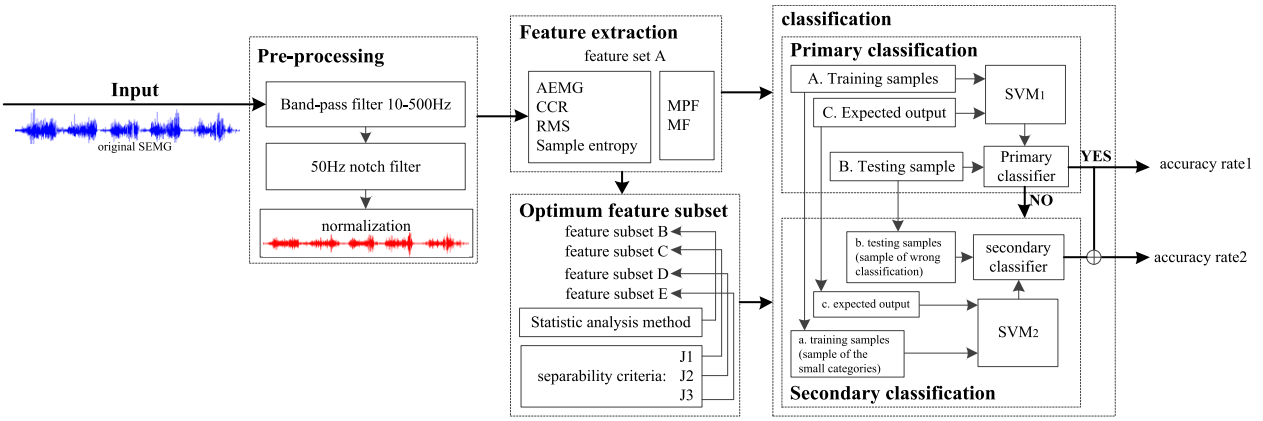

FIGURE 2. The proposed process model for CLBP recognition.

session of the experiment, sites of subject's skin where electrodes were attached was cleaned with alcohol to guarantee that the electrode-skin contact does not get contaminated. To reduce the ECG artifact in EMG signal, the center-to-center distance between the electrodes of each channel was made 20mm, which is the shortest possible distance. Finally, data were acquired at a sampling rate of 1000 Hz using a configurable electromyography (EMG) system (BioNomadix, BIOPAC Systems, Inc., USA).

C. PROCESS MODEL FOR CLBP RECOGNITION

SEMG signal acquired from the subjects are explored with the systemic process model shown in **Figure 2**. The model is designed to identify patients with CLBP from a given pool of LBP dataset. Raw sEMG signals received at the input node of the process model goes through pre-processing, feature extraction, optimal feature selection, and classification modules; all for the purpose of identifying subjects with CLBP. Details of each stage steps are presented in the following subsections.

1) SIGNAL PRE-PROCESSING

First, the signals acquired from each subject were passed to a 10-500 Hz band-pass filter to ensure that all components of the signals do not have frequencies outside the bandwidth of a typical range for sEMG signals. Subsequently, a 50 Hz-notch filter was applied to eliminate power frequency disturbances that could be present in the signal. Both filters were applied offline using the signal processing toolbox in MATLAB 2014a.

After filtering noise components in the signal, sEMG normalization was observed for a fair comparison between the acquired signals. Maximum voluntary contraction (MVC) is a commonly used method for sEMG normalization [32], [34]. The method involves rating the energy level of each subject based on the maximum contraction possible for a reference muscle. However, it might not be suitable for LBP subjects as the lumbar vertebra can be seriously hunted when trying to evaluate the maximum possible contraction [32]. Thus, an alternative approach, maximum value [35], was adopted in this study. This involves determining the maximum value (MV) of an sEMG signal for a distinct movement recorded from a subject and normalizing it to a unique range in which remaining parts of the signal are expressed as a percentage of the MV (%MV). This normalization method is used to ensure that a common ground is established when comparing the signal from all subjects irrespective of their LBP status. Thus, the respective data for each movement made by each subject were normalized based on the individual MV. Each data sample had a length of 16000 ms; however, data [20] with a length of 14000 ms was selected from each sample and processed further, as explained in the subsequent sections.

2) FEATURE EXTRACTION

Sequel to the filtering of unwanted components in the acquired signals and normalization, the features essential for LBP classification were extracted. To quantify the subjects' muscular activities, time and frequency domains parameters were obtained from normalized EMG signal of each subject. Six classes of features namely, average electromyogram, co-contraction ratio, root mean square, sample entropy mean power frequency and median frequency, were observed from the EMG signals obtained from the subjects. The first four classes are time domain feature, while mean power frequency and median frequency are features observed in frequency domain of the signal. The procedures taken to extract each feature class are explained below.

a: AVERAGE ELECTROMYOGRAM OF THE sEMG

Average electromyogram (AEMG) value reflects the innervation input from the sEMG signals acquired for all muscles that were activated during a certain movement. In this study, it is calculated as mean of amplitudes of sEMG signals that were acquired from the five trials for a given subject. The AEMG is a single-valued parameter that is not associated with time series of the sEMG signal. The value is derived

from the normalized sEMG signal, as given in Eq. 1.

$$\text{AEMG} = \frac{\sum_{i=1}^{N} |Data[i]|}{N} \tag{1}$$

b: CO-CONTRACTION RATIO OF MUSCLE

Muscle co-contraction is another important variable which can be used to assess the functions of lumbar muscles. In this study, co-contraction ratio is calculated as a normalized integration of the antagonistic sEMG activities divided by that of the total muscle activities. This is expressed with Eq.2.

$$\text{CCR} = \frac{AEMG_{anta}}{AEMG_a + AEMG_{anta}} \tag{2}$$

Where: CCR is the co-contraction ratio of the muscle activities; $AEMG_{anta}$ is the normalized integration of antagonistic muscle activities, and $AEMG_a$ is the normalized integration of agonistic muscle activities.

c: ROOT MEAN SQUARE OF THE sEMG

Root mean square (RMS) is used to evaluate the muscle force. This is defined as square root of the average sEMG signal that is acquired over a certain time period T . RMS of an acquired signal can be expressed with Eq. 3.

$$\text{RMS} = \sqrt{\frac{\sum_{i=0}^{T} sEMG[i]^2}{T}} \tag{3}$$

d: SAMPLE ENTROPY (SamEn)

Change in the complexity of sEMG signals captured during muscular activities can be observed and used for further processes. In this study, we explored the change in complexity of lumbar muscle activities by using the sample entropy (SamEn) of sEMG signals captured during the four different movements. Algorithmically, sample entropy (SamEn) of a recorded signal can be calculated as follows:

Given a time sequence data $\{(\text{i})\,\forall_{i=1,2,\ldots,K}\}$, where K is the total length of data, it is necessary to construct vectors of length m, defined as:

$$X_i = [x_i, x_{i+1}, \ldots x_{i+m-1}], \quad \forall i = 1, 2, \ldots, k-m+1 \tag{4}$$

Then, the probability that two vectors have similar number of data segments is calculated as:

$$Num_i\,(m, r) = \frac{num(d(X_i, X_j) \leq r)}{K - m + 1} \tag{5}$$

Where $num\left(d\left[X_i, X_j\right] \leq r\right)$ the number of similar data is segments between the two vectors X_i and X_j when the constraint modeled, as Eq. 6, is used. If the distance between the two vectors is less than parameter r, a pre-set constant value, a counter signifying the similarity weight between X_i and X_j is increased by one.

$$\text{d}\left[X_i, X_j\right] = \max_{\substack{h=0\sim m-1 \\ i\neq j}} |x\,(i+h) - x(j+h)| \leq r \tag{6}$$

Where $\text{d}\left[X_i, X_j\right]$ is the maximal absolute difference between vectors X_i and X_j in their respective scalar components; r specifies the filter level (tolerance). Then, the average probability over all the vectors in the data is calculated as:

$$A^m\,(r) = \frac{1}{K - m + 1} \sum_{i=1}^{K-m+1} Num_i\,(m, r) \tag{7}$$

Similarly, the process sequence was repeated for subseries of the signal at a fixed length of m + 1 to calculate $A^{m+1}\,(r)$. As a final step, SamEn of the signal can be given as:

$$\text{SamEn (m, r, K)} = -\ln \frac{B^{m+1}(r)}{A^m(r)} \tag{8}$$

To calculate the sample entropy, the parameters m and r are taken as constant values. Usually, the optimal value of m is 1 or 2; however, r has a range of values from 0.1SD to 0.25SD (SD is standard deviation of the time series) [36]. In this study, we selected values m = 2 and r = 0.15 for experiments.

e: MEAN POWER FREQUENCY (MPF) AND MEDIAN FREQUENCY (MDF) OF SURFACE ELECTROMYOGRAPHY

Aside the 4 time domain features explained above, we also used 2 frequency domain features to assess the strength of muscles. In the frequency domain, conduction velocity, Mean Power Frequency (MPF) and Median Frequency (MDF) are essential parameters for assessing the strength of muscles from recorded sEMG signals [31]; however, only the last two were used in this study. MPF is defined as the frequency location of average power in a spectrum. The MDF of a signal is a useful frequency that shows a power spectrum as two individual parts with the same dimension. For a given spectrum, the mean power frequency can be calculated as:

$$\text{MPF} = \frac{\int_0^{\infty} f_i \cdot PSD(f_i)df}{\int_0^{\infty} PSD(f_i)df} \tag{9}$$

Where f_i is the frequency of any arbitrary part in the power spectrum; and PSD is density of the power spectrum. Hung *et al.* [31] assumed a linear proportionality of the conduction velocity and applied it to determine the median frequency of a power spectrum, as related to muscle fatigue. Coefficient of the conduction velocity (v) is first evaluated with Eq. 10, then the MDF can be obtained with respect to other variables in the model.

$$v = (\frac{f_{MDF}}{f_{m0}})v_0 \tag{10}$$

Where f_{m0} is the initial MDF with $v = v_0$. The condition with conduction velocity at its initial reflects fatigue of the muscle, and this can be utilize describe presence of CLBP. Hence, MDF can be used for fatigue compensation and spectral analysis for CLPB evaluation. This is described as:

$$\int_0^{MDF} PSD(f)df = \int_{MDF}^{\infty} PSD\,(f)\,df = \frac{1}{2}\int_0^{\infty} PSD(f)df \tag{11}$$

The co-contraction ratio (CCR) is a single value evaluated as the normalized integration of antagonistic sEMG activities to that of total muscle activities, over the six different muscles. The other five features, described in previous section, were evaluated by each of the muscles. Thus, each subject can be characterized by thirty-one features which were applied for subsequent processing.

3) OPTIMAL FEATURE SELECTION

Sequel to calculating the thirty-one features, a selection method is needed to select the important features (inputs) from the original feature set for constructing a reliable CLBP classifier with better performance. Procedure for feature selection had two fundamental aspects namely, a criterion of selection and a procedure of search [37], [38]. Of the feature selection methods in signal processing, sequential feature selection (SFS) is mostly used for their speed [39]. SFS algorithm is a bottom-up search procedure that starts with an empty set and features are gradually added upon passing some evaluation functions [40]. In this study, it is used to estimate the accuracy of a support vector machine (SVM) classifier defined on three criteria (J1, J2, J3). Selection is based on differences between two particular features in different subjects, and the classification error from the four types of movements considered in this study. At each iteration, an individual feature is selected from the pool of available features and added to a feature-set being put together for classification. So, the newly extended set, which is a subset of the original feature-set, is compared with another that is subset made-up of dissimilar features. Finally, the subset of features that produces best classification with minimum error is selected. This algorithm takes the whole d-dimensional feature-set $\mathrm{M} = \{m_1, m_2, \ldots\ldots, m_d\}$ as input. The optimal feature-set starts as an empty set $X_n = \emptyset$, and $n = 0$. Each feature (m_i) is tested added into the set. Thus, at each i^{th} iteration, the optimal feature-set is as follow:

$$X_n = \left\{x_j \,|\, j = 1, 2, 3, \ldots, n; x_j \in M\right\} \tag{12}$$

Where $\mathrm{n} = 1, 2, 3, \ldots, d$ and $n < d$. The next best feature x^+, is sequentially selected with Eq. 13, with $n := n + 1$.

$$\begin{aligned} x^+ &= \text{argmax}\, J\left(x_n + x\right) \\ X_{n+1} &= X_n + x^+ \end{aligned} \tag{13}$$

Where $x \in \mathrm{M} - X_n$. This procedure is repeated until a termination criterion is satisfied. The three criteria proposed for this purpose: J1, J2, and J3; are defined based on the distance formulae given in Eq. 14-16.

$$J_1\left(X\right) = tr(S_w^{-1} S_b) \tag{14}$$

$$J_2\left(X\right) = \frac{tr(S_b)}{tr(S_w)} \tag{15}$$

$$J_3\left(X\right) = \frac{|S_w + S_b|}{S_w} \tag{16}$$

Where tr is the trace of a matrix; while S_w and S_b is the within-class and between-class scatter matrix, respectively.

4) CLBP CLASSIFICATION METHOD

Upon successful selection of the optimal features, the CLBP entities in the dataset are identified with based on support vector machine (SVM). SVM is a supervised learning method that uses machine learning algorithm for solving classification and prediction problems. Classifiers built based on SVM create maximum-margin hyperplane(s) that lies in a transformed input space and splits entities in the space into different classes. Compared with artificial neural network models, SVM generally has better performance in handling small datasets [41], [42]; thus, SVM classification method is developed for CLBP recognition, in this study. We assume a data sample of the format: $(\mathrm{X}_1, \mathrm{y}_1)$, $(\mathrm{X}_2, \mathrm{y}_2)$, ∘, $(\mathrm{X}_n, \mathrm{y}_n)$, $\boldsymbol{X} \in \boldsymbol{R}^d$ and $\mathrm{y}_1 \in \{-1, 1\}$ as separable by a hyper-plane with chosen functions of the form:

$$(\mathbf{W} \cdot \boldsymbol{X}) + b = 0 \mathbf{W} \epsilon R^d, b \epsilon \boldsymbol{R} \tag{17}$$

$$f\left(\boldsymbol{X}\right) = sgn((\mathbf{W} \cdot \boldsymbol{X}) + b) \tag{18}$$

Where W is weight; X is input vector; and b is the bias. Thus, a corresponding decision function can be modeled as Eq. 18. To solve this, we need an optimal hyperplane that divides all samples into two classes with minimal distance to margin. This problem of optimal classification-plane can be transformed into an optimization problem, expressed in Eq. 19. To solve the optimization problem under a certain constraint, the Lagrangian function in Eq. 20 are introduced with multipliers $\alpha_i \geq 0$ to achieve a solution vector.

$$\begin{aligned} &\text{minQ}\left(\boldsymbol{\alpha}\right) = \frac{1}{2} \sum_{i,j=1}^{n} \alpha_i \alpha_j y_i y_j K\left(X_i, X_j\right) - \sum_{i=1}^{n} \alpha_i \\ &\text{s.t. } \alpha_i \geq 0 \quad (i = 1, 2, \ldots, \mathrm{n}) \\ &\qquad \sum_{i=1}^{n} y_i \alpha_i = 0 \end{aligned} \tag{19}$$

$$\mathrm{L}\left(\mathbf{W}, b, \boldsymbol{\alpha}\right) = \frac{1}{2} \|\mathbf{W}\|^2 - \sum_{i=1}^{n} \alpha_i (y_i \cdot ((\mathbf{W} \cdot X_i) + b) - 1) \tag{20}$$

Thereby, the equation of optimal classification-plane can be represented with Eq. 21, with the dataset satisfying $|g(\boldsymbol{X})| = 1$. This indicates the distance to margin is minimal, and thus, the dataset is a support vector are the patterns that correspond with the nonzero multipliers α_i called the support values. $\mathrm{g}\left(\boldsymbol{X}\right) = (\mathbf{W} \cdot \boldsymbol{X}) + b$ is the general form of the linear discriminant function in d dimensional space.

$$f\left(x\right) = y_i = sgn\left(\sum_{i=1}^{n} \alpha_i^* y_i \left(X_i, X_j\right) + b\right) \tag{21}$$

The hyperplane decision function presented in Eq. 18 can now be solved from the a set of support vectors with values $\alpha_i \neq 0$. Choice of the support vector are then used to calculate b^* in Eq. 21, as Eq. 22, thus we have the classification output.

$$b = \frac{i}{|I|} \sum_{i=1}^{n} \left(y_i - \sum_{j=1}^{n} \alpha_j^* y_j \left(X_i, X_j\right)\right)_{i \in I} \tag{22}$$

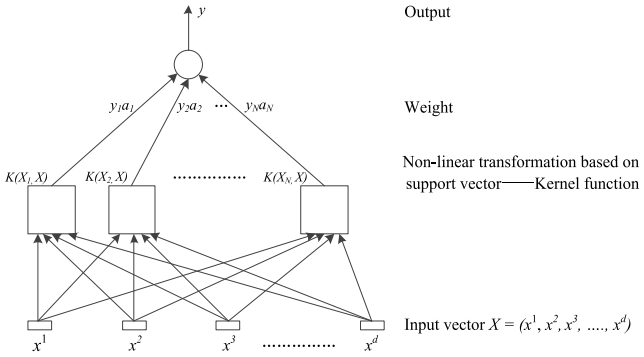

FIGURE 3. The structure diagram of SVM classification on data sets.

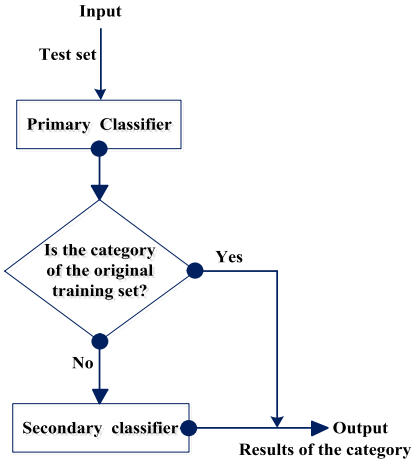

FIGURE 4. Flow chart of the category homogenizing method.

Model of an SVM classifier is illustrated in **Figure 3**. Despite the fact that most of the subjects with CLPB have almost similar features, a few of them were found to be somewhat different. This is called uneven distribution, an inherent feature in data processing which has been said to lower accuracy when using supervised classification methods [43]. To minimize this effect, equalization of samples amongst the classes of a training dataset is necessary. To achieve this, we applied a category homogenizing method better classification. Entities (subjects) in the small classes are combined to form a bigger class and ordered based on feature similarities. The resulting bigger is, of course, different from the other category having a high magnitude in the original data. This process yields a new training data with two distinct classes with even entity distribution, and it was used to build classifiers. Therefore, this involves building two different SVM classifiers namely, SVM1 and SVM2 on the new training data. Then, the recognition accuracy of the CLBP classification scheme is evaluated on the testing data. As an initial and default step, a sample is first recognized with SVM1 to check if he/she is has CLBP, and the classification result is compared with the actual status, as in the health record. This is regarded as primary classification, and most of the samples are classified correctly with it; thus, SVM1 is tagged as primary classifier. Nevertheless, there are a few cases where the classification result from SVM1 is wrong. Such sample instance is sent for retry in SVM2 to check if he/she can be recognized as having CLBP or if truly he/she does not have the lower back pain condition. Thus, SVM1 is tagged as secondary classifier, and the classification process ends with it. **Figure 4** is a flow chart of the classification process based on the category homogenizing method, discussed above.

III. RESULTS

Eighty-eight patients with CLBP aged 21-50 (mean 35.56, SD = 7.28) and eighty-three healthy subjects aged 24-49 (mean 34.27, SD = 5.87), were recruited. The population has a gender percentage of 77.19% female and 22.81% male, in the subject pool. From each subject, we collected sEMG data from six muscles of interest and extracted the thirty-one time and frequency domain features each for four different movements. Thus, the dataset has a dimension of 171x31x4, which is a total of 21204 tuples to be explored. For proper analysis, each of the thirty-one feature was numbered as given in **Table 2**. In this study, the statistical method was applied

TABLE 2. Number and name of thirty-one feature set (The number of each feature is applied to four types of movement).

Feature number	**1**	**2**	**3**	**4**	**5**	**6**	**7**
Name	AEMG of left LM	AEMG of right LM	AEMG of left EO	AEMG of right EO	AEMG of left IO/TrA	AEMG of right IO/TrA	CCR
Feature number	**8**	**9**	**10**	**11**	**12**	**13**	**14**
Name	RMS of left LM	RMS of right LM	RMS of left EO	RMS of right EO	RMS of left IO/TrA	RMS of right IO/TrA	SamEn of left LM
Feature number	**15**	**16**	**17**	**18**	**19**	**20**	**21**
Name	SamEn of right LM	SamEn of left EO	SamEn of right EO	SamEn of left IO/TrA	SamEn of right IO/TrA	MPF of left LM	MPF of right LM
Feature number	**22**	**23**	**24**	**25**	**26**	**27**	**28**
Name	MPF of left EO	MPF of right EO	MPF of left IO/TrA	MPF of right IO/TrA	MDF of left LM	MDF of right LM	MDF of left EO
Feature number	**29**	**30**	**31**				
Name	MDF of right EO	MDF of left IO/TrA	MDF of right IO/TrA				

to obtain features with significant differences, and feature selection methods were applied to find the optimal feature subset from the 31 features. These were done to improve accuracy of the SVM classifiers for the purpose of CLPB recognition.

A. ANALYSIS OF SUBJECT GROUP FOR THE FOUR MOVEMENT TYPES

To demonstrate differences in the subject groups for each of the movement, statistical analysis were performed by comparing the CLBP subjects and healthy controls based one feature, at a time. The analysis involves carrying out *Wilcoxon test* for each of the thirty-one features, listed in **Table 2**. The Wilcoxon test is a non-parametric statistical hypothesis test used to compare two samples that their means are not the same. It is an alternative to the t-test thus, it is used for dependent samples when population cannot be assumed to be normally distributed [44]. In the analysis, subjects groups were examined based on the AEMG and RMS values, CCR measurements, sample entropy, MPF and MDF as obtained for their muscular activities. The results obtained, upon analyzing each of the four movements, are shown in **Figure 5**.

As presented in **Figure 5(a)**, analysis of the features obtained when subjects in both the CLBP group and the healthy control carried out forward bending movements. It can be seen that fifteen of the features, those with numbers #(5, 16-21, 23, 24, 26-31), shows significant difference ($p < 0.05$) between two groups for the forward bending movement. Specifically, the CLBP group shows more features with lower values than those in the healthy controls when for the specific movement. Similarly, analysis of the features obtained from the two groups for backward bending movement is shown as **Figure 5b**. Unlike in the forward bending movement, only nine features indicate significant differences between the CLBP subjects and healthy controls. The specific features are #(4, 14, 17, 18, 25, 28-31), and the features have higher values for the CLBP subjects when compared to the healthy controls. Also, an analysis of the features obtained from the two groups for left lateral flexion is shown as in **Figure 5c**. Six specific features namely, #(18, 20, 24, 26, 30, 31) show significant differences with the of the CLBP group having higher values that the healthy controls. Lastly, for the right lateral flexion, the CLBP group shows significant differences with nine features having lower values than controls, as shown in **Figure 5(d)**. The particular parameters are #(5, 12, 18, 20, 21, 23, 24, 26, 30). Analyses of **Figure 5** show that some features are more useful for CLBP recognition. Thus, CLBP recognition in different subjects cannot always be handled with a specific feature set during different movements.

B. ANALYSIS OF OPTIMAL FEATURE SELECTION

Greater dynamics is involved when it comes to deciding the best features that can yield higher accuracy in CLBP recognition. Thus, the SFS method was used to select the best discriminative features in the feature selection stage of the proposed process model in **Figure 1**. As explained in Section 2, three criteria J1, J2 and J3 were defined for selecting optimal feature subsets that can be uniquely utilized for the four movements. Some specific feature subsets considered for classification purpose in this study, are presented in **Table 3**. Evolutions of the classification accuracy and mean squared error analyzed for the different feature subsets, based on the criteria J1, J2, and J3, are shown in **Figure 6.**

Evolution of the classification accuracy and error based on selection criterion J1, J2 and J3 for forward bending movement are shown in **Figure 6a and 6a'**. We found that 7 of the 31 features namely #(30, 29, 26, 31, 27, 24, 20), were optimal by using the criterion J1 for SFS in the forward movement, while criterion J2 and J3 return 28 features, namely #(30, 2, 1, 5, 8, 9, 3, 4, 12, 6, 10, 11, 13, 7, 18, 16, 17, 15, 14, 19, 29, 21, 20, 31, 28, 23, 27, 26), and 6 features namely #(30, 29, 20, 24, 27, 31) as the optimal subset of the 31 features. A careful analysis of the figures that shows the optimal feature subset yielded the highest classification accuracies and minimum classification errors, respectively. Similarly,

TABLE 3. Obtained feature subset after applying criteria J1, J2, J3 of the SFS method.

Movements	Selection criterion	No. of optimal feature subset	Size of a full set of features	Optimal subset
Forward bending	J1	7	31	#(30,29,26,31,27,24,20)
	J2	28	31	#(30,2,1,5,8,9,3,4,12,6,10,11,13,7,18,16,17,15,14,19,29,21,20,31,28,23,27,26)
	J3	6	31	# (30,29,20,24,27,31)
Backward bending	J1	23	31	#(30,7,9,1,3,6,4,5,2,23,19,26,31,16,10,11,29,15,17,27,20,24,28)
	J2	25	31	# (30,4,1,5,7,3,6,11,2,8,12,13,10,9,18,14,15, 16,17,19,31,28,23,25,29)
	J3	14	31	# (30,7,9,1,3,4,6,5,2,31,23,27,29,21)
Left lateral flexion	J1	29	31	#(23,7,10,12,8,6,4,2,18,14,21,16,31,28,29,11,17,9,3,19,30,24,5,15,27,1,13,26,22)
	J2	31	31	#(23,2,7,5,1,9,4,6,12,13,8,11,3,10,14,18,15,17,19,16,22,30,25,21,20,24,31,26,29,27,28)
	J3	26	31	# (23,7,10,12,30,8,21,6,4,2,18,14,31,16,26,24, 29,11,17,9,27,1,28,22,3,5)
Right lateral flexion	J1	12	31	# (30,24,20,26,8,12,22,21,27,2,7,13)
	J2	31	31	#(30,3,1,5,2,4,10,8,12,11,9,6,13,7,18,15,14,16,17,19,20,22,21,26,28,23,29,31,24,25,27)
	J3	12	31	# (30,24,20,26,8,12,22,21,27,9,7,13)

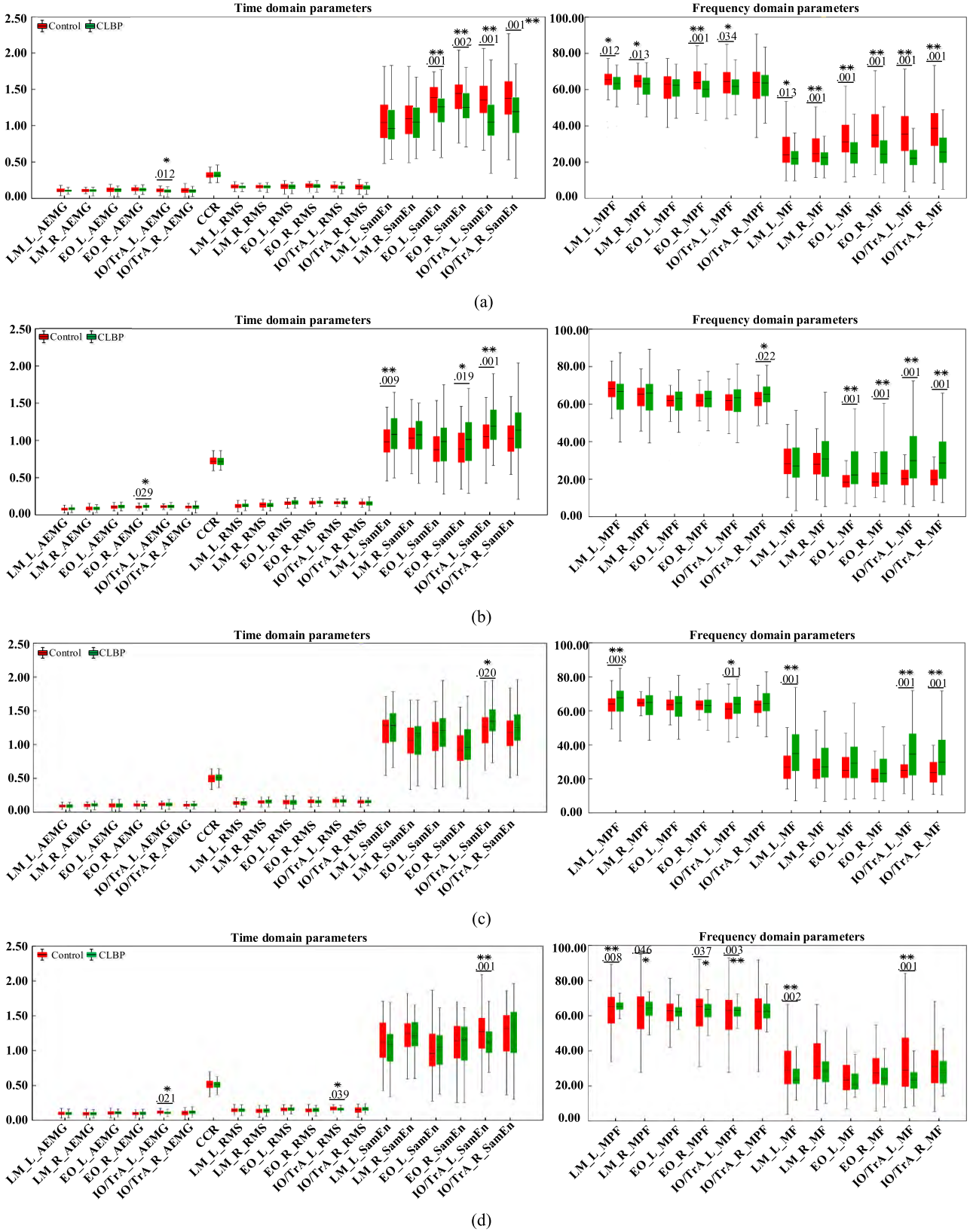

FIGURE 5. Boxplot of thirty-one characteristic from CLBP group and healthy control group for each type of movement considered in this study. (* significant difference ($p < 0.05$) between CLBP and control groups. ** significant at 0.01 level). (a) Forward bending movement, (b) backward bending movement, (c) left lateral flexion, and (d) right lateral flexion.

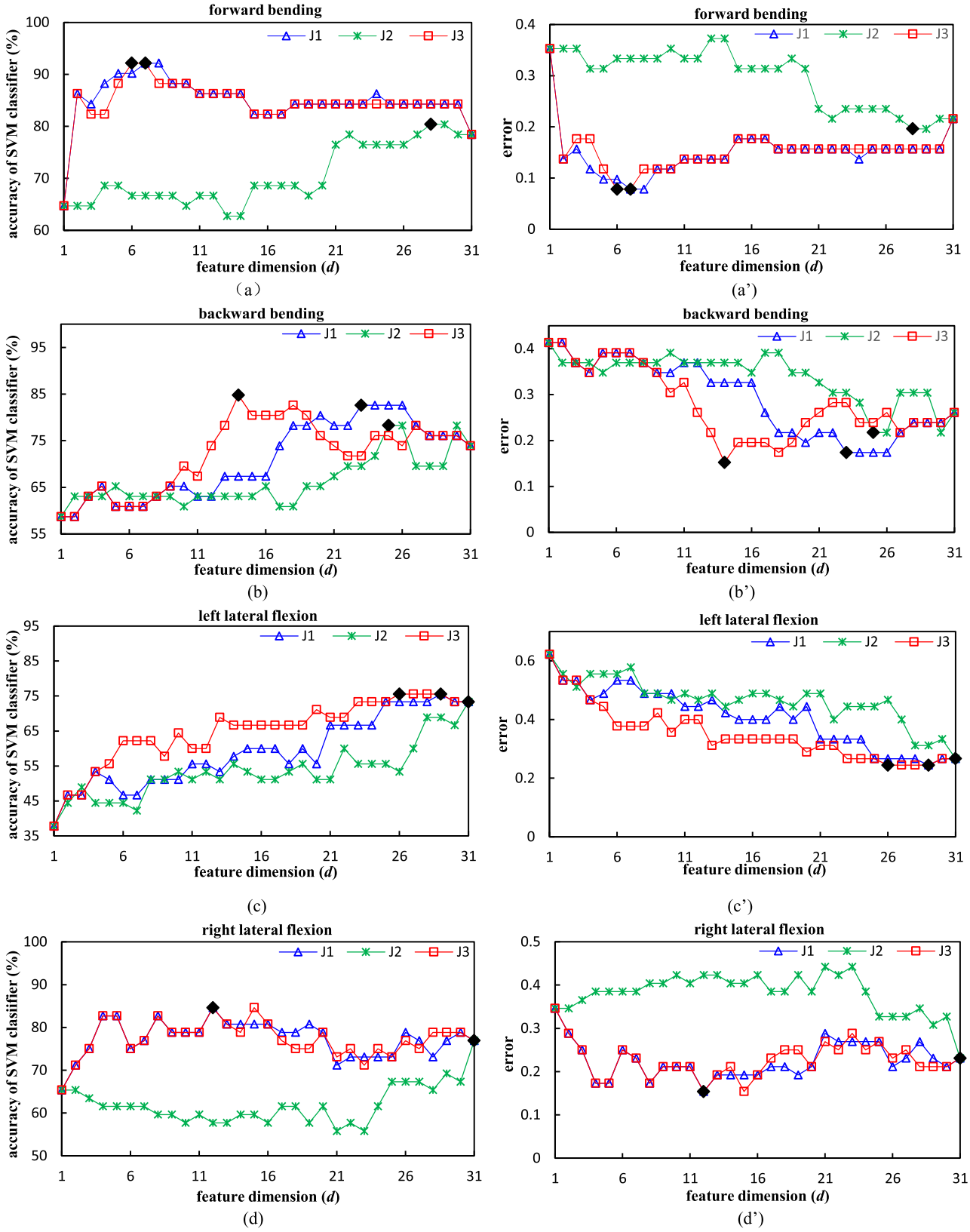

FIGURE 6. The accuracy and mean squared error of SVM classification of the optimum feature combination based on three separability criteria J1, J2 and J3. (a) forward bending movement, (b) backward bending movement, (c) left lateral flexion movement, and (d) right lateral flexion movement. The right column shows the mean squared error corresponding to criteria J1, J2, and J3 during (a')-(d') four type of movement.

classification results for backward bending movement based on the three criteria are shown in **Figure 6b and 6b'**. Evaluation of the backward bending movement shows that optimal subset of the 31 features were #(30, 7, 9, 1, 3, 6, 4, 5, 2, 23, 19, 26, 31, 16, 10, 11, 29, 15, 17, 27, 20, 24, 28), that is 23 features, when criterion J1 was used, while criterion J2 returned 25 features namely #(30, 4, 1, 5, 7, 3, 6, 11, 2, 8, 12, 13, 10, 9, 18, 14, 15, 16, 17, 19, 31, 28, 23, 25, 29), and criterion J3 of the SFS showed that 14 features, which are #(30, 7, 9, 1, 3, 4, 6, 5, 2, 31, 23, 27, 29, 21), as the optimal feature subset.

Correspondingly for left lateral flexion movement, the highest classification accuracy were achieved with 29 features namely, #(23, 7, 10, 12, 8, 6, 4, 2, 18, 14, 21, 16, 31, 28, 29, 11, 17, 9, 3, 19, 30, 24, 5, 15, 27, 1, 13, 26, 22), 31 features namely # (23, 2, 7, 5, 1, 9, 4, 6, 12, 13, 8, 11, 3, 10, 14, 18, 15, 17, 19, 16, 22, 30, 25, 21, 20, 24, 31, 26, 29, 27, 28), and 26 features namely #(23, 7, 10, 12, 30, 8, 21, 6, 4, 2, 18, 14, 31, 16, 26, 24, 29, 11, 17, 9, 27, 1, 28, 22, 3, 5), as the optimal subsets based on selection criteria J1, J2, and J3, respectively. Classification performance for the three criteria are shown in plots of **Figure 6c and 6c'**. Lastly, for right lateral flexion movement data set, 12, 31, and 12 features namely #(30, 24, 20, 26, 8, 12, 22, 21, 27, 2, 7, 13), #(30, 3, 1, 5, 2, 4, 10, 8, 12, 11, 9, 6, 13, 7, 18, 15, 14, 16, 17, 19, 20, 22, 21, 26, 28, 23, 29, 31, 24, 25, 27), and #(30, 24, 20, 26, 8, 12, 22, 21, 27, 9, 7, 13), respectively, gave the highest classification performance accuracy based on selection criteria J1, J2, J3, respectively. These are as illustrated in plots d and d' of **Figure 6**.

C. CLBP RECOGNITION BASED ON THE ORIGINAL FEATURE SET AND ITS SUBSETS

Finally, the proposed process model is evaluated by exploring data with different feature sets for CLBP recognition. This involves analyzing the classification performance of a model based on datasets generated during the four types of movement with five different feature sets. The feature sets are described as:

a) *Feature-set A*: the normalized dataset characterized with all the thirty-one features;
b) *Feature subset B:*the normalized dataset characterized by only the features with a significant difference between the CLBP subjects and healthy controls. This was obtained by performing the Wilcoxon-test on the dataset;
c) *Feature subset C:* the normalized dataset characterized with features obtained based on criterion J1 of SFS method;
d) *Feature subset D:* the normalized dataset characterized with features obtained based on criterion J2 of SFS method;
e) *Feature subset E:*the normalized dataset characterized with features obtained based on criterion J3 of SFS method.

The specific classification results based on each feature set are presented for both the primary and secondary classifiers in **Figure 7**. Plot (a) shows that feature subset C achieved highest accuracy (at 98.04%) for CLBP recognition during forward bending movement while with feature set A, subset B, subset D, and subset E, slightly lower accuracies of 96.08%, 94.12%, 94.12% and 96.08%, respectively, were obtained for the CLBP recognition during the same movement. However, for backward bending movement, the feature subset B gave a recognition rate of 91.30% for CLBP using the dataset. Nonetheless, other feature set A, subset C, subset D, subset E achieved accuracies of 89.13%, 84.78%, 84.78% and 89.13%, respectively, for CLBP recognition; these are slightly lower when compared with that of feature subset B for the same movement.

In the same way, feature subset D and subset E returned a similar accuracy of 93.33% for CLBP recognition, which is the highest recognition accuracy obtained from the five feature sets during left lateral flexion movement. Slightly lower accuracies of 88.89%, 88.89% and 91.11%, respectively, were recorded with other feature sets, that is set A, subset B, and subset C when used for the same movement. Lastly, for right lateral flexion movement, feature subset E recorded a slightly higher accuracy of 96.15% for CLBP recognition when compared with feature set A, subset B, subset C, and subset D which achieved accuracies of 90.38%, 92.31%, 88.46% and 94.23%, respectively, for the CLBP recognition.

For each plot in **Figure 7**, the results of both primary (blue) and secondary (red) classifiers are displayed. It is clear that for the four types of movement, the classification accuracy of the secondary classifier is more stable and better compared to that of the primary classifier. Thus, it is essential to clarify that the highest accuracy observed to describe the recognition performance, in the last paragraph, are values of the secondary classifier; and having a hybrid of SVM classifiers adds to the accuracy of the CLBP classification for each of the movement.

For a better understanding of the readers, the values plotted for both classifiers in **Figure 7** are tabulated as **Table 4**. In addition, the relationship between the feature subset with significant difference and the optimal subsets obtained based on criteria J1, J2, J3 of SFS method are analyzed and plotted as shown in **Figure 8**. The plots show that all features in subset B are always contained in feature subset D for the four types of movements except for feature # 24: MPF of left IO/TrA which is an additional feature in subset B for forward bending movement. However, the corresponding feature subset C and E only included part feature subset B for the four types of movements, respectively.

IV. DISCUSSION

CLBP recognition based on sEMG signal could be a promising alternative to diagnoses of patients with non-specific back pain disorders or pathology rather than using conventional approaches, such as medicine, epidural injection, or even

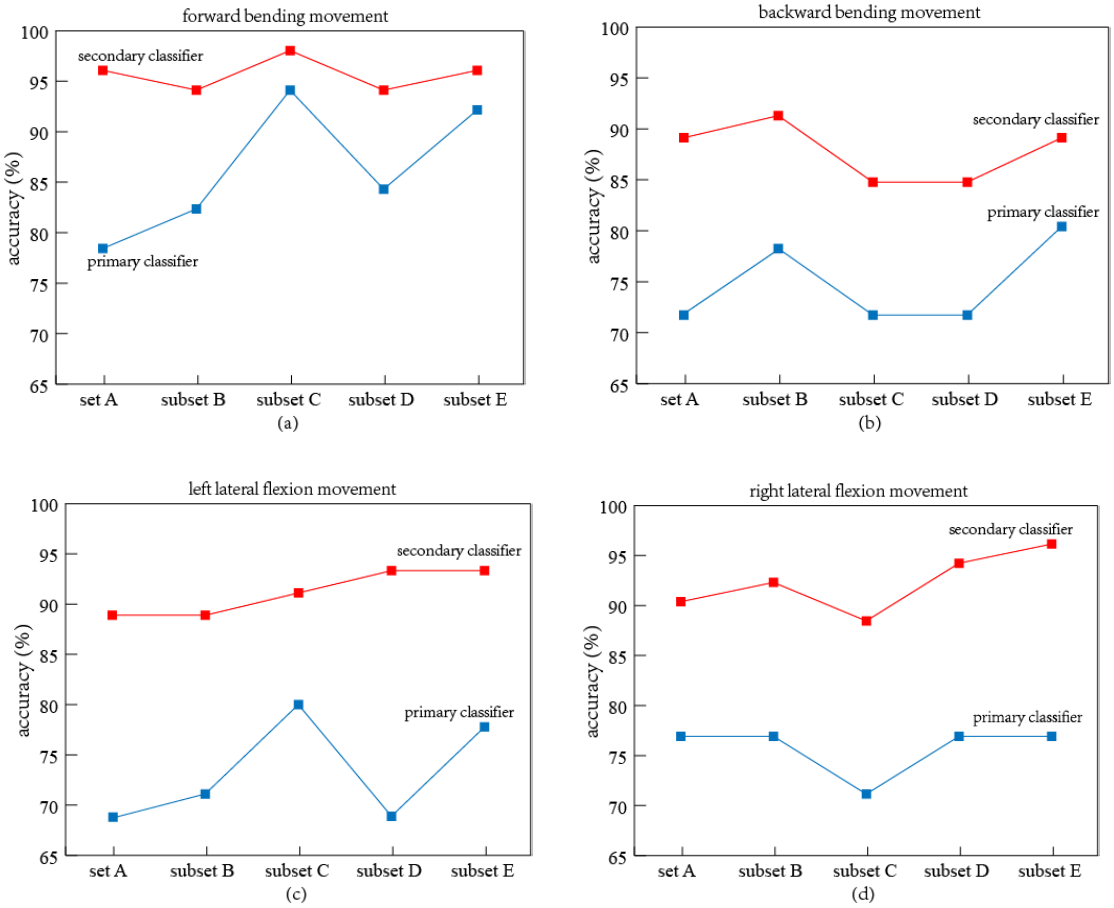

FIGURE 7. The accuracy of CLBP recognition was calculated based on different feature set A, subset B, C, D, and E during four types of movement. (a) forward bending movement, (b) backward bending movement, (c) left lateral flexion movement, and (d) right lateral flexion movement.

TABLE 4. Result of CLBP recognition based on different feature set and subset during four types of movement.

Movements	SVM	Set A (%)	Subset B (%)	Subset C (%)	Subset D (%)	Subset E (%)
Forward bending movement	Primary classifier	0.7843	0.8235	0.9412	0.8431	0.9216
	Secondary classifier	0.9608	0.9412	**0.9804**	0.9412	0.9608
Backward bending movement	Primary classifier	0.7174	0.7826	0.7174	0.7174	0.8043
	Secondary classifier	0.8913	**0.9130**	0.8478	0.8478	0.8913
Left lateral flexion movement	Primary classifier	0.6889	0.7111	0.8000	0.6889	0.7778
	Secondary classifier	0.8889	0.8889	0.9111	0.9333	**0.9333**
Right lateral flexion movement	Primary classifier	0.7692	0.7692	0.7115	0.7692	0.7692
	Secondary classifier	0.9038	0.9231	0.8846	0.9423	**0.9615**

spinal surgery. In this study, we have carried out experiments to explore several features of lumbar muscles during four different types of movement namely, forward bending, backward bending, left lateral flexion, and right lateral flexion. For CLBP recognition, thirty-one representative features were explored from sEMG signals acquired from each subject. The features include nineteen time domain features of AEMG, RMS, CCR, SamEn parameters and twelve frequency domain features of MPF, MDF parameters. In the experimental study, SFS selection method was applied to identify optimal feature subsets for each of the four movements, and the results obtained shows that the highest accuracy of CLBP recognition during each of the four movements. For instance, in forward bending movement, 98.04% accuracy was obtained with the secondary classifier when feature subset C was used, while feature subset B gave the highest CLBP recognition accuracy (91.30%) in the case of backward bending movement. Similarly, the highest accuracy of CLBP recognition

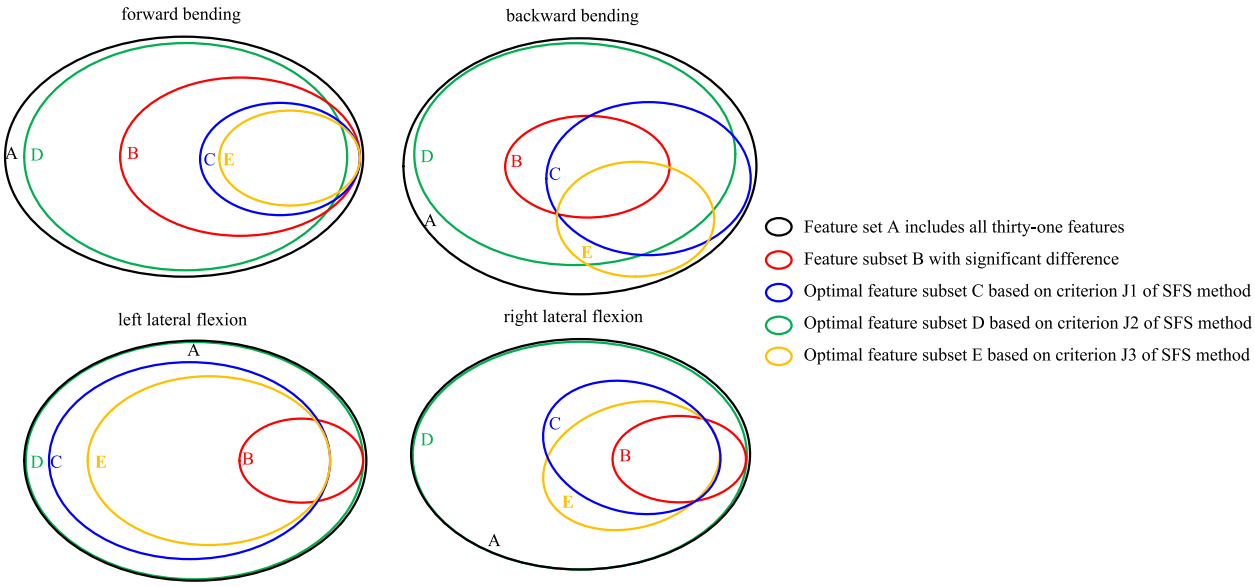

FIGURE 8. The relationship between different features set A, subset B, C, D, and E during four types of movement.

for left lateral flexion was 93.33%, and this was obtained by both feature subset D and subset E, which is a unique case in the four movements. Correspondingly, feature subset E gave the highest accuracy of CLBP recognition for right lateral flexion was 96.15%.

SFS selection is an essential process for good CLBP recognition system. The process could help reduce an overload of using many features which at times are not necessary and could incur extra computation resources. An instance is the high number of features that overlap between feature subset B and subset D for the four types of movements explored in this study. That is, except for feature #24: MPF of left IO/TrA which is the only difference between the two feature subsets and just in the case of forward bending movement, all other features in the two subsets are the same after feature selection. Specifically, in forward bending movement, the CLBP recognition accuracy of the secondary classifier base on subset B and subset D are both 94.12%. Thus, this indicates that the complement feature of the subset B found in the subset D are not vital for CLBP recognition during the forward bending movement. However, for backward bending, the accuracies of CLBP recognition based on subset B and subset D are 91.30% and 84.78%, respectively. Thus, it shows that features in subset D that are not present in subset B reduces the recognition accuracy of CLBP in the subjects.

Similarly, for both lateral flexion, the accuracy of CLBP recognition based on subset B is greater than that of subset D. This indicates that the extra features in subset D are quite important for optimal CLBP recognition in the subjects. Therefore, the statistical analysis shows that the feature subset B can reveal significant information ($p < 0.05$) of dysfunction signs and symptoms suffered by patients with CLBP, while the feature subset D would seem to include a lot of information which might not be revealed out by the signs and symptoms used for diagnosis of the chronic pain. Moreover, subsets C and E only included a few parts of subset B for the four movements explored in this study. This indicates that features of subset B with statistical significance seems not to play significant roles for subsets C and E in CLBP recognition. Hence, studies on the disease recognition can analyze as many as possible features but should only carefully consider only those features with clinical and statistical significance as they will enhance the classification performance, better.

It is important to emphasize that activities of the lumbar muscles depend on different types of spinal tractions actuated to ensure balanced postures that are required for coordinating human body procedures between muscles and bones for daily physical activities [45]. The present study provides clear evidence that the AEMG, RMS, SamEn, MPF and MDF values of left IO/TrA muscle are lower for forward bending and right lateral flexion movement, and are higher for backward bending and left lateral flexion movement in CLBP participants compared to those of the healthy controls (at a statistical significance level $p < 0.05$). In fact, trends in AEMG and RMS values of muscles presented in this study explains insufficient activation or over-activation of muscles necessary for lumbar spine stabilization. Differences in muscle contraction could cause Sample entropy to be reduced or increased. Lower contraction tends to be maintained in slight oscillatory mode due to smaller values of Sample entropy, while higher muscle activities tend to produce greater sample entropy values which can lead to complex oscillatory spine mode [46]. Similarly, MPF and MDF are the most useful and popular frequency-domain features for the assessment of muscle strength [47]; thus, MPF and MDF of IO/TrA muscle in

CLBP participants are characterized during the movements. MPF and MDF were lower in CLBP participants because of reduced muscular forces as a result of pains from secretion from inflammations in the lumbar spine, patient's psychological disorders or motor control dysfunction [26], [48]. Thus, under the condition of insufficient muscular strength, stress-dependent muscular activities, maladaptive cognitions and suppressive thoughts may lead to a long-lasting overloading of muscles and joints; thus, causing LBP [49], [50].

Specifically, the AEMG value of patients with CLBP reduced in forward bending movement because the activation of IO/TrA muscle is insufficient while the lower sample entropy of the muscle in the subject group can be explained with weak oscillatory modes in the muscle recruitment compared to that of the healthy controls. Also, lower values of MPF and MDF in the CLBP subjects reflect the weak IO/TrA muscle strength during the forward bending movement. Furthermore, AEMG value of the CLBP subjects increased for backward bending movement because EO muscle was over-activated to maintain the lumbar spine stability demand, while the increased sample entropy of EO muscle found in the group may be as a result of complex oscillatory modes. Similarly, higher sample entropy and increased MPF and MDF of IO/TrA muscle are found in CLBP participants also during left lateral flexion movement. Thus, increased MDF value of EO muscle could be as a high muscle strength needed. Conversely, AEMG and RMS value of IO/TrA muscle reduced in the CLBP subjects for right lateral flexion movement. This could be due to the fact that IO/TrA muscle was not sufficiently activated causing slightly oscillatory modes which, in turn, leads to lower sample entropy of IO/TrA muscle and reduced MPF and MDF value of IO/TrA, compared to those of healthy controls. Hence, these indicate that, muscle contraction and oscillatory strength are different for each of the four movements. As a result, feature subset is said to be influenced by selective movement while recognition accuracy depends greatly on the selected feature (sub) set.

To analyze the functions of individual muscles, the present study also shows that the left IO/TrA muscle is more critical during three of the four movements namely, forward bending, left and right lateral flexion, when with the other five muscles. However, the right EO_R muscle is quite vital than the other five muscles for backward bending movement due to the statistical difference between the subject groups. As a result, left IO/TrA muscle of CLBP subjects is more susceptible to damage than the other muscles when performing the three movements while the right EO muscle is more susceptible to such dysfunction during the backward movement [29]. The analysis confirms that many altered activation pattern in the deep (TrA) muscle of CLBP patients indicates motor control dysfunction [51]. Similarly, improved side specific control of IO/TrA muscle could highlight improve motor control following exercise in people with CLBP [52]. Abdominal muscles such as internal oblique/transverse abdominis play an essential role in maintaining lumbar spine stability against the effects of gravity during delicate movements [53]. The present study provides clear evidence that activation pattern of IO/TrA changes in CLBP subjects compared to healthy controls; and that dysfunction of IO/TrA muscle activities could occur when performing forward bending, left and right lateral flexion movements, while dysfunction of EO muscle activities is only inherent with backward bending movement. Hence, these indicate that IO/TrA and EO muscles performed insufficient or over-activation to satisfy spine stability demands. Thus, as part of therapy for CLBP subjects, rehabilitation program with protected and strengthened function of IO/TrA and EO muscle should be considered. This will minimize the risk of augmenting LBP problems. It is paramount to advise CLBP subjects to strengthen the function of IO/TrA and EO muscles and not to perform complicated exercises to improve dysfunction of the lumbar spine.

As discussed above, evaluation of AEMG, sample entropy, MPF, and MDF in the CLBP and healthy control groups appeared to reveal the difference of muscle activation and oscillatory mode between CLBP and healthy controls. Hence, feature subset B based on statistical analysis and optimal feature subset C, D, E based on criteria J1, J2, J3 of SFS method would seem to recognize some mechanical causes of lumbar spinal dysfunction effectively. We implemented the process model as a computerized system for diagnosis of CLBP in patients with non-specific pathology using SVM classifiers. This could be useful in detecting the risk factors of CLBP based on different muscle activation and oscillatory patterns. Furthermore, the approach may be considered for improved cognitive, behavioral, emotional management of subjects with CLBP in order to avoid deadlier pathological conditions such as spinal stenosis or herniated disks.

V. CONCLUSION AND FUTURE WORK

The main objective of this study is to recognize CLBP based on feature set A, subset B, C, D, and E during four types of movement namely: forward bending, backward bending, left lateral flexion and right lateral flexion. For each movement made by each subject, 31 features, consisting of nineteen time domain and twelve frequency domain features, were calculated and used as feature set for CLBP recognition. Statistical differences and feature selection methods were applied to categorize the 31 features into five different sets, including the original feature set. To avoid the influence of uneven sample distribution, as a result of little dataset, on recognition accuracy, two SVM classifiers, tagged as primary and secondary, were used for the CLBP recognition. This study shows that having a secondary SVM classifier improved the CLBP recognition accuracy compared to using only the primary classifier, and the highest accuracy of CLBP recognition was 98.04% based on feature subset.

It is important to note that this study is limited in terms of the number of subjects recruited. A total of only 171subjects, out of which 88 were CLBP patients, were available for the study. Also, patients with complicated CLBP condition were not considered to avoid the possibility of damaging their lumbar spine while performing the movements designed

for this study. Also, all subjects were asked to ensure stable amplitude during the four types of movements. However, there were still some variations in the amplitude achieved by each subject. In the future, a larger dataset will be acquired for multi-level CLBP classification based on machine learning tools such as deep learning, to control CLBP. Thus, subjects with complicated CLBP condition could be considered.

REFERENCES

[1] O. Airaksinen *et al.*, "European guidelines for the management of chronic nonspecific low back pain," *Eur. Spine J.*, vol. 15, no. 3, pp. 192–300, 2006.

[2] C. M. Filley, H. Burke, and C. A. Anderson, "Anterior cerebral artery territory infarction-related resolution of chronic lower back pain," *J. Neuropsychiatry Clin. Neurosci.*, vol. 30, no. 1, pp. 81–83, 2018.

[3] V. Mohan, A. Paungmali, and P. Sitilertpisan, "The science of respiratory characteristics in individuals with chronic low back pain: Interpreting through statistical perspective," *J. Bodywork Movement Therapies*, vol. 22, no. 1, pp. 11–12, 2018.

[4] V. Y. Ma, L. Chan, and K. J. Carruthers, "Incidence, prevalence, costs, and impact on disability of common conditions requiring rehabilitation in the United States: Stroke, spinal cord injury, traumatic brain injury, multiple sclerosis, osteoarthritis, rheumatoid arthritis, limb loss, and back pain," *Arch. Phys. Med. Rehabil.*, vol. 95, no. 5, pp. 986–995, 2014.

[5] M. de G. Salvetti, C. A. Pimenta, P. E. Braga, and C. F. Corrôa, "Disability related to chronic low back pain: Prevalence and associated factors," *Revista Da Escola De Enfermagem Da USP*, vol. 46, pp. 16–23, Oct. 2012.

[6] P. Bodera, W. Stankiewicz, B. Kalicki, J. Kieliszek, J. Sobiech, and A. Krawczyk, "The surface electromyography biofeedback in pain management—Theoretical assumptions and possibilities of using the method," *Przeglad Elektrotechniczny*, vol. 88, no. 12B, pp. 115–116, 2012.

[7] G. C. Miyamoto, C. C. Lin, C. M. N. Cabral, J. M. van Dongen, and M. W. van Tulder, "Cost-effectiveness of exercise therapy in the treatment of non-specific neck pain and low back pain: A systematic review with meta-analysis," *Brit. J. Sports Med.*, 2018, doi: 10.1136/bjsports-2017-098765.

[8] A. Ahlqwist and C. Sällfors, "Experiences of low back pain in adolescents in relation to physiotherapy intervention," *Int. J. Qualitative Stud. Health Well-Being*, vol 7, no. 1, 2012, Art. no. 15471.

[9] S. Angel, L. D. Jensen, B. K. Gonge, T. Maribo, B. Schiøttz-Christensen, and N. Buus, "Patients' interpretations of a counselling intervention for low back pain: A narrative analysis," *Int. J. Nursing Stud.*, vol. 49, no. 7, pp. 784–792, 2012.

[10] E. Mathew, E. Kim, and W. Zempsky, "Pharmacologic treatment of pain," *Seminars Pediatric Neurol.*, vol. 23, no. 3, pp. 209–219, 2016.

[11] R. B. North, J. Shipley, H. Wang, and N. Mekhail, "A review of economic factors related to the delivery of health care for chronic low back pain," *Neuromodulation*, vol. 17, no. 3, pp. 69–76, 2014.

[12] L. Manchikanti, V. Pampati, A. D. Kaye, and J. A. Hirsch, "Therapeutic lumbar facet joint nerve blocks in the treatment of chronic low back pain: Cost utility analysis based on a randomized controlled trial," *Korean J. Pain*, vol. 31, no. 1, pp. 27–38, 2018.

[13] J. D. Childs *et al.*, "Implications of early and guideline adherent physical therapy for low back pain on utilization and costs," *BMC Health Services Res.*, vol. 15, p. e150, Apr. 2015.

[14] J. M. Fritz, G. P. Brennan, S. J. Hunter, and J. S. Magel, "Initial management decisions after a new consultation for low back pain: Implications of the usage of physical therapy for subsequent health care costs and utilization," *Arch. Phys. Med. Rehabil.*, vol. 94, no. 5, pp. 808–816, 2013.

[15] A. Chuck, W. Adamowicz, P. Jacobs, A. Ohinmaa, B. Dick, and S. Rashiq, "The willingness to pay for reducing pain and pain-related disability," *Value Health*, vol. 12, no. 4, pp. 498–506, 2009.

[16] M. Gore, A. Sadosky, B. R. Stacey, K. S. Tai, and D. Leslie, "The burden of chronic low back pain: Clinical comorbidities, treatment patterns, and health care costs in usual care settings," *Spine*, vol. 37, no. 1, pp. E668–E677, 2012.

[17] J. Alleva, T. Hudgins, J. Belous, and A. Origenes, "Chronic low back pain," *DM Disease -A- Month*, vol. 62, no. 9, pp. 330–333, 2016.

[18] A. Obbarius, N. Obbarius, F. Fischer, G. Liegl, S. Nolte, and M. Rose, "Evaluating different patterns of chronic pain through PROs-applying latent class analysis to visual analogue scales," *Qual. Life Res.*, vol. 26, no. 1, p. 24, 2017.

[19] H. Breivik, "Fifty years on the Visual Analogue Scale (VAS) for pain-intensity is still good for acute pain. But multidimensional assessment is needed for chronic pain," *Scand. J. Pain*, vol. 11, pp. 150–152, Apr. 2016.

[20] A. S. Saariaho, T. H. Saariaho, A. K. Mattila, M. Karukivi, and M. Joukamaa, "Alexithymia and early maladaptive schemas in chronic pain patients," *Scand. J. Psychol.*, vol. 56, no. 4, pp. 428–437, 2015.

[21] C. A. Mancuso *et al.*, "Successful lumbar surgery results in improved psychological well-being: A longitudinal assessment of depressive and anxiety symptoms," *Spine J.*, vol. 18, no. 4, pp. 606–613, 2018.

[22] L. Guarda-Nardini, C. Pavan, N. Arveda, G. Ferronato, and D. Manfredini, "Psychometric features of temporomandibular disorders patients in relation to pain diffusion, location, intensity and duration," *J. Oral Rehabil.*, vol. 39, no. 10, pp. 737–743, 2012.

[23] S. Bergman, "Management of musculoskeletal pain," *Best Pract. Res. Clin. Rheumatol.*, vol. 21, no. 1, pp. 153–166, 2007.

[24] M. Hasenbring, D. Hallner, and B. Klasen, "Psychological mechanisms in the transition from acute to chronic pain: Over- or underrated?" *Schmerz*, vol. 15, no. 6, pp. 442–447, 2001.

[25] D. Viggiani and J. P. Callaghan, "Hip abductor fatigability and recovery are related to the development of low back pain during prolonged standing," *J. Appl. Biomech.*, vol. 34, no. 1, pp. 39–46, 2018.

[26] S. Zhang, Y. Xu, X. Han, W. Wu, Y. Tang, and C. Wang, "Functional and morphological changes in the deep lumbar multifidus using electromyography and ultrasound," *Sci. Rep.*, vol. 8, Apr. 2018, Art. no. 6539.

[27] B. Bazrgari and T. Xia, "Application of advanced biomechanical methods in studying low back pain—Recent development in estimation of lower back loads and large-array surface electromyography and findings," *J. Pain Res.*, vol. 10, pp. 1677–1685, Jul. 2017.

[28] P. Tyagi, A. S. Arora, and V. Rastogi, "Stress analysis of lower back using EMG signal," *Biomed. Res.*, vol. 28, no. 2, pp. 519–524, 2017.

[29] T. Suehiro, H. Ishida, K. Kobara, H. Osaka, and S. Watanabe, "Altered trunk muscle recruitment patterns during lifting in individuals in remission from recurrent low back pain," *J. Electromyogr. Kinesiol.*, vol. 39, pp. 128–133, Apr. 2018.

[30] D. Goubert, J. V. Oosterwijck, M. Meeus, and L. Danneels, "Structural changes of lumbar muscles in non-specific low back pain: A systematic review," *Pain Physician*, vol. 19, no. 7, pp. E985–E1000, 2016.

[31] C. C. Hung, T. W. Shen, C. C. Liang, and W. T. Wu, "Using surface electromyography (SEMG) to classify low back pain based on lifting capacity evaluation with principal component analysis neural network method," in *Proc. IEEE Eng. Med. Biol. Soc. Conf.*, 2014, pp. 18–21.

[32] W. Du, H. Li, O. M. Omisore, L. Wang, W. Chen, and X. Sun, "Co-contraction characteristics of lumbar muscles in patients with lumbar disc herniation during different types of movement," *Biomed. Eng. Online*, vol. 17, no. 8, p. 8, 2018.

[33] N. W. Willigenburg, I. Kingma, and J. H. van Dieën, "Center of pressure trajectories, trunk kinematics and trunk muscle activation during unstable sitting in low back pain patients," *Gait Posture*, vol. 38, no. 4, pp. 625–630, 2013.

[34] M. Behrens, A. Mau-Moeller, S. Heise, R. Skripitz, R. Bader, and S. Bruhn, "Alteration in neuromuscular function of the plantar flexors following caffeine ingestion," *Scand J. Med. Sci. Sports*, vol. 25, no. 1, pp. e50–e58, 2015.

[35] M. Halaki and K. Ginn, *Normalization of EMG Signals: To Normalize or Not to Normalize and What to Normalize to?* Rijeka, Croatia: Intech, 2012, ch. 7, pp. 176–194.

[36] M. Aboy, D. Cuesta-Frau, D. Austin, and P. Mico-Tormos, "Characterization of sample entropy in the context of biomedical signal analysis," in *Proc. IEEE 29th Annu. Int. Conf. Eng. Med. Biol. Soc.*, Piscataway, NJ, USA, Aug. 2007, pp. 5942–5945.

[37] R. Chen, N. Sun, X. Chen, M. Yang, and Q. Wu, "Supervised feature selection with a stratified feature weighting method," *IEEE Access*, vol. 6, pp. 15087–15098, 2018.

[38] C. Deng *et al.*, "Enhancing the discrimination ability of a gas sensor array based on a novel feature selection and fusion framework," *Sensors*, vol. 18, no. 6, p. E1909, 2008.

[39] S. Bouatmane, M. A. Roula, A. Bouridane, and S. Al-Maadeed, "Round-robin sequential forward selection algorithm for prostate cancer classification and diagnosis using multispectral imagery," *Mach. Vis. Appl.*, vol. 22, no. 3, pp. 865–878, 2011.

[40] H. Ghayab, Y. Li, S. Abdulla, M. Diykh, and X. Wan, "Classification of epileptic EEG signals based on simple random sampling and sequential feature selection," *Brain Informat.*, vol. 3, no. 2, pp. 85–91, 2016.

[41] X. Ju and Y. Tian, "A divide-and-conquer method for large scale v-nonparallel support vector machines," *Neural Comput. Appl.*, vol. 29, no. 9, pp. 497–509, 2018.
[42] Z. Wang, Z. Zhou, Y. Chen, X. Li, and Y. S. Sun, "Support vector machines model of computed tomography for assessing lymph node metastasis in esophageal cancer with neoadjuvant chemotherapy," *J. Comput. Assist. Tomography*, vol. 41, no. 3, pp. 455–460, 2017.
[43] J. Gong, J. Y. Liu, X. W. Sun, B. Zheng, and S. D. Nie, "Computer-aided diagnosis of lung cancer: The effect of training data sets on classification accuracy of lung nodules," *Phys. Med. Biol.*, vol. 63, no. 3, p. 035036, 2018.
[44] A. T. Darilay and J. D. Naranjo, "A pretest for using logrank or Wilcoxon in the two-sample problem," *Comput. Statist. Data Anal.*, vol. 55, no. 7, pp. 2400–2409, 2011.
[45] J. Kang and I. Hyong, "Changes in electromyographic activity of lumbar paraspinal muscles according to type of inverted-spinal-traction," *Wireless Pers. Commun.*, vol. 93, no. 1, pp. 35–45, 2017.
[46] E. Y. Suda, P. Madeleine, R. P. Hirata, A. Samani, T. T. Kawamura, and I. C. Sacco, "Reduced complexity of force and muscle activity during low level isometric contractions of the ankle in diabetic individuals," *Clinical Biomech.*, vol. 42, pp. 38–46, Feb. 2017.
[47] J. H. van Dieën, J. Cholewicki, and A. Radebold, "Trunk muscle recruitment patterns in patients with low back pain enhance the stability of the lumbar spine," *Spine*, vol. 28, no. 8, pp. 834–841, 2003.
[48] W. Li *et al.*, "Diagnosis of compressed nerve root in lumbar disc herniation patients by surface electromyography," *Orthopaedic Surg.*, vol. 10, no. 1, pp. 47–55, 2018.
[49] M. Russo *et al.*, "Muscle control and non-specific chronic low back pain," *Neuromodulation*, vol. 21, no. 1, pp. 1–9, 2018.
[50] M. Chang, L. V. Slater, R. O. Corbett, J. M. Hart, and J. Hertel, "Muscle activation patterns of the lumbo-pelvic-hip complex during walking gait before and after exercise," *Gait Posture*, vol. 52, pp. 15–21, Feb. 2017.
[51] S. P. T. ShahAli *et al.*, "Ultrasound measurement of abdominal muscles during clinical isometric endurance tests in women with and without low back pain," *Physiotherapy Theory Pract.*, vol. 26, pp. 1–9, Feb. 2018.
[52] M. F. Knox, L. S. Chipchase, S. M. Schabrun, and P. W. M. Marshall, "Improved compensatory postural adjustments of the deep abdominals following exercise in people with chronic low back pain," *J. Electromyogr. Kinesiol.*, vol. 37, pp. 117–124. Dec. 2017.
[53] Y.-S. Kong, S. Park, M.-G. Kweon, and J.-W. Park, "Change in trunk muscle activities with prone bridge exercise in patients with chronic low back pain," *J. Phys. Therapy Sci.*, vol. 28, no. 1, pp. 264–268, 2016.

WENJING DU received the M.S. degree from the Electronic Engineering and Automation Department, Guilin University of Electronic Technology, Guilin, China, in 2016. Since 2016, she has been an Assistant Researcher with the Shenzhen Institutes of Advanced Technology, Chinese Academy of Sciences, Shenzhen, China. Her research interests include biomedical signal processing and medical ultrasound.

OLATUNJI MUMINI OMISORE received the B.Tech. and M.Tech. degrees in computer science from the Federal University of Technology, Akure, Nigeria, in 2009 and 2014, respectively. He is currently pursuing the Ph.D. degree with the Shenzhen Institutes of Advanced Technology, Chinese Academy of Sciences, China. He was a Research Assistant/Software Engineer with HTRDG Computers Ltd., Akure, from 2010 to 2014. In 2014, he joined Oduduwa University Ipetumodu, Ile-Ife, Nigeria, where he was an Assistant Lecturer. In 2014, he moved to the Centre for Information Technology and Systems, University of Lagos, Nigeria, where he was a System Analyst until 2015. He has authored/co-authored more than 35 scientific papers, including 10 SCI/EI indexed articles, 2 monographs, and 15 IEEE/ACM conference papers. His research interests include surgical robotics (automation and control), computational intelligence, and digital libraries with specialty in data and knowledge mining.

HUIHUI LI received the B.S. and M.S. degrees from Shenzhen University, Shenzhen, China, in 2003 and 2006, respectively, and the Ph.D. degree from Xi'an Jiaotong University, Xi'an, China, in 2011. Since 2012, she has been an Assistant Professor with the Shenzhen Institutes of Advanced Technology, Chinese Academy of Sciences, Shenzhen. She has authored over 10 articles. Her research interests include biomedical signal processing, medical ultrasound, and miniature antenna design.

KAMEN IVANOV received the B.Sc. degree from the Technical University of Sofia, Bulgaria, in 2003. He is currently pursuing the Ph.D. degree in biomedical electronics engineering with the Shenzhen Institutes of Advanced Technology, Chinese Academy of Sciences, Shenzhen, China. His research interests include medical instrumentation and biomedical signal processing.

SHIPENG HAN received the B.Eng. degree in mechanical engineering from the Shaanxi University of Technology, Hanzhong, China, in 2014, and the M.Eng. degree in mechanical engineering from Guizhou University, Guiyang, China, in 2017. He was an Intern Student with the Research Centre for Medical Robotics and MIS Devices, Shenzhen Institutes of Advanced Technology, Chinese Academy of Sciences, Shenzhen, China, from 2015 to 2017. He is currently a Research Assistant in surgical robotics (machine design and control) with the Shenzhen Institutes of Advanced Technology, Chinese Academy of Sciences. He has authored/co-authored over 10 SCI/EI papers and engineering patents.

LEI WANG received the B.Eng. degree in information and control engineering and the Ph.D. degree in biomedical engineering in 1995 and 2000, respectively. He was with the University of Glasgow and Imperial College London, from 2001 to 2008. He is currently with the Shenzhen Institutes of Advanced Technology, Chinese Academy of Sciences, as a Professor and the Deputy Director with the Institute of Biomedical and Health Engineering. He has published over 200 scientific papers and authored 10 books/book chapters. He holds 30 patents. His research interests include body sensor networks.